The Astrophysical Journal, 956:1 (6pp), 2023 October 10 https://doi.org/10.3847/1538-4357/acf767

Is a Recently Discovered H I Cloud near M94 a Starless Dark Matter Halo?

Alejandro Benitez-Llambay[1] and Julio F. Navarro[2]
[1] Dipartimento di Fisica G. Occhialini, Università degli Studi di Milano Bicocca, Piazza della Scienza, 3 I-20126 Milano MI, Italy
alejandro.benitezllambay@unimib.it
[2] Department of Physics and Astronomy, University of Victoria, Victoria, BC V8P 5C2, Canada
Received 2023 August 8; revised 2023 September 4; accepted 2023 September 5; published 2023 September 29

Abstract

Observations with the Five-hundred-meter Aperture Spherical Telescope have revealed the presence of a marginally resolved source of 21 cm emission from a location $\sim 50'$ from the M94 galaxy, without a stellar counterpart down to the surface brightness limit of the DESI Imaging Legacy Survey ($\sim$29.15 mag arcsec^{-2} in the g band). The system (hereafter Cloud-9) has round column density isocontours and a line width consistent with thermal broadening from gas at $T \sim 2 \times 10^4$ K. These properties are unlike those of previously detected dark H I clouds and similar to the expected properties of REionization-Limited-H I Clouds (RELHICs), namely, starless dark matter (DM) halos filled with gas in hydrostatic equilibrium and in thermal equilibrium with the cosmic ultraviolet background. At the distance of M94, $d \sim 4.7$ Mpc, we find that Cloud-9 is consistent with being a RELHIC inhabiting a Navarro–Frenk–White (NFW) DM halo of mass $M_{200} \sim 5 \times 10^9\ M_\odot$ and concentration $c_{\rm NFW} \sim 13$. Although the agreement between the model and observations is good, Cloud-9 appears to be slightly, but systematically, more extended than expected for ΛCDM RELHICs. This may imply either that Cloud-9 is much closer than implied by its recessional velocity, $v_{\rm CL9} \sim 300$ km s^{-1}, or that its halo density profile is flatter than NFW, with a DM mass deficit greater than a factor of 10 at radii $r \lesssim 1$ kpc. Further observations may aid in constraining these scenarios better and help elucidate whether Cloud-9 is the first ever observed RELHIC, a cornerstone prediction of the ΛCDM model on the smallest scales.

Unified Astronomy Thesaurus concepts: Cosmology (343); Reionization (1383); Dark matter (353)

1. Introduction

A distinctive prediction of the Lambda-Cold Dark Matter (ΛCDM) model of structure formation is the existence of a vast number of collapsed halos, whose density follows a universal profile (Navarro–Frenk–White (NFW), Navarro et al. 1996), and whose abundance at the low-mass end scales as a power law of the mass, $\propto M^{-1.9}$ (e.g., Press & Schechter 1974; Bond et al. 1991; Jenkins et al. 2001; Angulo et al. 2012; Wang et al. 2020). This result, combined with the relatively flat faint end of the galaxy luminosity function, implies that a large population of low-mass dark matter (DM) halos must remain "dark" or starless until the present day (see, e.g., Ferrero et al. 2012, and references therein).

The origin of these "dark" halos in the ΛCDM is well motivated theoretically: galaxies can only form in the center of halos whose mass exceeds a redshift-dependent critical mass, $M_{\rm crit}(z)$. This critical mass corresponds, before cosmic reionization, to the halo mass above which atomic cooling becomes efficient (e.g., Blumenthal et al. 1984; Bromm & Yoshida 2011), and, after reionization, to the halo mass above which the pressure of the photoheated gas cannot overcome the gravitational force of the halo (Benitez-Llambay & Frenk 2020, hereafter BLF20).

Analytical models (Ikeuchi 1986; Rees 1986; Benitez-Llambay & Frenk 2020) and results from hydrodynamical simulations (e.g., Hoeft et al. 2006; Okamoto et al. 2008; Benítez-Llambay et al. 2017), demonstrate that DM halos less massive than $M_{\rm crit} \sim 7 \times 10^9\ M_\odot$ today should contain gas in hydrostatic equilibrium with the gravitational potential of the halo and in thermal equilibrium with the external ultraviolet background radiation (UVB). Moreover, the models indicate that halos that never exceeded $M_{\rm crit}(z)$ should remain devoid of stars to the present day.

For the most massive "dark" halos, the high density and low temperature of their gas lead to the formation of neutral hydrogen (H I) in the center, making them detectable in 21 cm emission. This is why these systems were termed "REionization-Limited-H I-Clouds" (RELHICs) by Benítez-Llambay et al. (2017, hereafter BL17), and are analogs of the minihalos envisaged by Rees (1986) and Ikeuchi (1986) in the context of the early Lyα forest models.

The properties of RELHICs in ΛCDM were studied by BL17. The authors concluded that RELHICs should be nearly spherical extragalactic gas clouds in hydrostatic equilibrium with the underlying NFW halo. Their gas density profile is well specified because of the distinctive density–temperature relation that arises from the interplay between gas cooling and photoheating. As RELHICs are close to hydrostatic equilibrium, they lack significant velocity dispersion.

Detecting RELHICs would represent a remarkable achievement mainly for two reasons. Above all, it would unequivocally confirm the presence of bound collapsed DM structures on mass scales below galaxies, a pivotal prediction of the ΛCDM model. Second, it would pave the way toward a novel and independent way to probe ΛCDM on small scales, where ΛCDM is still subject to heavy scrutiny (see, e.g., Bullock & Boylan-Kolchin 2017 for a recent review of the small-scale challenges faced by ΛCDM).

As discussed by BL17, the most promising RELHIC candidates to date have been some of the Ultra Compact High-Velocity Clouds (UCHVCs) identified in the ALFALFA catalog (Adams et al. 2013; Haynes et al. 2018). This catalog contains roughly 60 "dark" H I clouds whose sizes and fluxes are broadly consistent with RELHICs. Of these candidates, the

systems that appear round in the sky display either a large broadening of their H I line compatible with nonzero velocity dispersion (or rotation) or negative recessional velocity, indicating they are likely nearby sources. On the other hand, H I clouds receding from us and having a small line-width broadening display a highly irregular morphology. Thus, no observational analog entirely consistent with RELHICs has been positively identified to date.

In this work, we focus on the discovery by Zhou et al. (2023, hereafter Z23) of extended emission in an isolated field near M94. The system (termed Cloud-9, hereafter CL-9) was observed with the Five-hundred-meter Aperture Spherical Telescope (FAST), has no obvious luminous counterpart, and exhibits properties consistent with those expected for RELHICs. Using the models introduced by BL17 and BLF20, we address whether the Z23 observations are consistent with CL-9 being a ΛCDM RELHIC. We refer interested readers to those papers for further details.

2. Method

2.1. Observations

Recently, Z23 reported the detection of CL-9, a relatively isolated H I cloud without a luminous counterpart brighter than the surface brightness limit of the DESI Legacy Imaging Survey (DESI LS), namely, 29.15, 28.73, and 27.52 mag arcsec^{-2} for the g, r, and z filters, respectively (Martínez-Delgado et al. 2023). The system is at a projected angular distance $\sim 51\farcm87$ from the center of M94, a galaxy located at a distance $d \sim 4.66$ Mpc (e.g., Lee et al. 2011). This value is broadly consistent with the distance obtained from its radial velocity, $v_{\rm M94} \sim 287$ km s^{-1}, assuming it is receding from us on the Hubble flow. Other distance estimates for M94 also place the galaxy in the distance range $4 \lesssim d/{\rm Mpc} \lesssim 5$ (e.g., Karachentsev et al. 2004; Crook et al. 2007; Cappellari et al. 2011; Tully et al. 2016; Karachentsev et al. 2018).

CL-9 has a recessional velocity similar to that of M94, $v_{\rm CL9} \sim 300$ km s^{-1} (Z23). This coincidence, together with the close angular separation, makes it likely that CL-9 is in the vicinity of M94. Assuming this is the case, the projected distance between CL-9 and M94 corresponds to a physical separation greater than ∼70 kpc and to a maximum stellar mass for CL-9, $M_{\rm str} \lesssim 10^5\ M_\odot$, as reported by Z23.

If CL-9 is not near M94, then its recessional velocity makes it unlikely that the system is closer than 3 Mpc from us. Indeed, no galaxies with a reliable distance estimate closer than 3 Mpc have recessional velocities that reach this value (see, e.g., Karachentsev & Kaisina 2019).

This lower bound on the distance is further supported by the distance estimate based on the velocity field reconstruction of the local volume using CosmicFlows-3 (Tully et al. 2016), which returns a distance in the range $3 \lesssim d/{\rm Mpc} \lesssim 4$. The lower/higher value is obtained when the reconstruction uses the numerical action method (Shaya et al. 2017)/Wiener filter model (Graziani et al. 2019).[3] However, it is not possible to exclude the possibility that CL-9 is farther than M94 using the system's recessional velocity alone.

CL-9 appears round in the sky and displays a narrow broadening of its emission line ($W_{50} \sim 20$ km s^{-1} at its peak column density), consistent with thermal broadening arising from gas at $T \sim 2 \times 10^4$ K. These properties are consistent with those expected for RELHICs (BL17). We note, however, that the inferred shape of CL-9 may be affected by the large FAST beam, the size of which is comparable to the spatial extent of the detection.

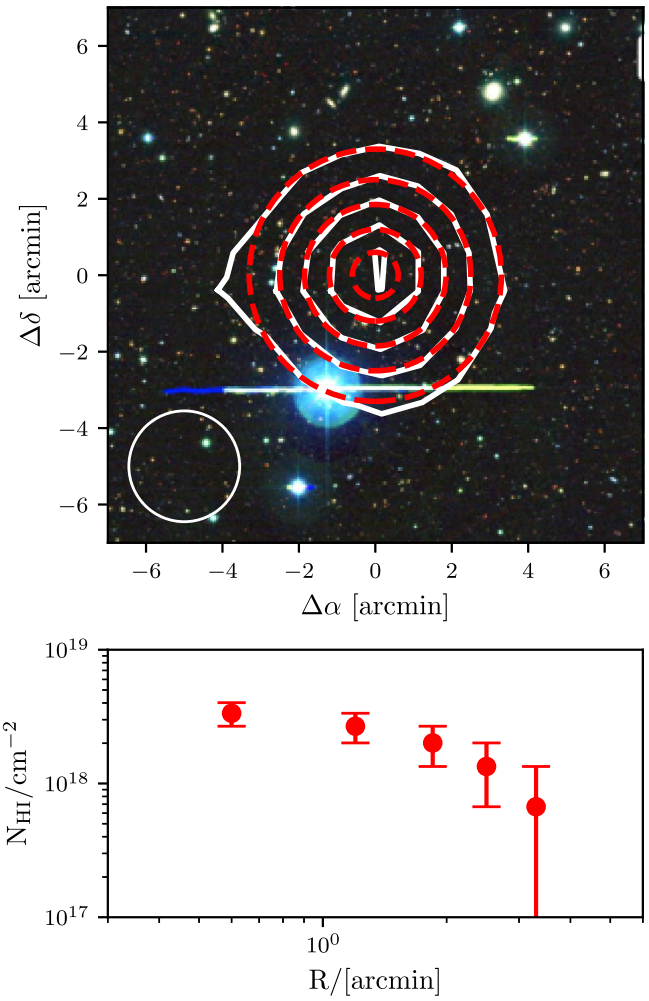

Figure 1. CL-9's observed column density isocontours (taken from Z23) superimposed on a DESI LS color image of the same field. The white circle indicates the FAST beam size. We approximate the observed isocontours with the dashed circles to construct the observed column density profile displayed in the bottom panel. The error bars indicate 3σ uncertainties. The coordinates are relative to the origin, $(\alpha, \delta) = (12^{\rm h}51^{\rm m}52^{\rm s}, +40°17'29'')$.

CL-9 is unlikely to be a self-gravitating system. If the system's sound-crossing time equals the free-fall time within the observed range, then the required H I mass for the system to be in equilibrium (given its line width and size at the distance of M94) is $M_{\rm HI} \sim 4 \times 10^8\ M_\odot$. This value is orders of magnitude higher than the derived H I mass given its total flux ($M_{\rm HI} \sim 7 \times 10^5\ M_\odot$) (Z23), implying the presence of a large amount of gravitational mass other than neutral hydrogen.

We show CL-9's observed column density isocontours, taken from the work of Z23, in the top panel of Figure 1. Following Z23, we superimpose the contours over a DESI LS color image to emphasize that there is no obvious extended luminous counterpart within the surface brightness limit of the survey.[4] The outermost isocontour corresponds to a value equal

[3] We queried the distance using the CosmicFlows-3 calculator available at http://edd.ifa.hawaii.edu (Kourkchi et al. 2020).

[4] Note that the presence of a bright star near CL-9 may somewhat affect the exact surface brightness limit reached by the DESI LS image at this location.

to the 3σ detection limit, $N_{\rm HI} = 6.7 \times 10^{17}$ cm^{-2}, and the contour values increase in steps of 6.7×10^{17} cm^{-2}, so that the maximum column density reached by the innermost contour is $N_{\rm HI} = 3.35 \times 10^{18}$ cm^{-2}.

Because the system's isocontours are round, we approximate them by the circles depicted by the dashed lines and use the circles' radii to produce the column density profile shown by the red dots in the bottom panel of Figure 1. Since the innermost isocontour is elliptical, we will not use it for our analysis.

2.2. RELHICs

2.2.1. Intrinsic Column Density Profile and Mock Observations

We model RELHICs following BL17. This implies assuming that RELHICs are spherical gaseous systems in hydrostatic equilibrium with an NFW DM halo and in thermal equilibrium with a Haardt & Madau (2012) UVB. We note that the presence of a stellar counterpart does not affect the structure nor the system's stability, provided the stars are negligible contributors to the gravitational potential.

To solve the hydrostatic equilibrium equation, we use a boundary condition where the pressure at infinity equals the pressure of the intergalactic medium at the mean density of the Universe. With this condition, the model reproduces the detailed structure of stable gaseous halos in large high-resolution cosmological hydrodynamical simulations (BL17, BLF20). In this model, RELHICs are characterized by a distinctive maximum central density, which depends on the gas temperature, halo virial mass, M_{200}, and concentration, $c_{\rm NFW}$.

To derive the H I density profile of RELHICs, we apply the Rahmati et al. (2013) results. Once the H I density profile is known, we calculate the intrinsic H I column density by projecting the H I density.

To compare Z23 observations with a RELHIC model, we place RELHICs at the observed distance and convolve their intrinsic column density profile with a circular Gaussian beam with standard deviation, $\sigma_{\rm beam} = 1\farcm23$, whose FWHM matches that of the FAST beam, $\sim 2\farcm9$. Performing this convolution is crucial because we will compare models with observations on scales smaller than the FAST beam size. Moreover, at the M94 distance, the angular extent of the central H I core of RELHICs is comparable to the beam size.

3. Results

3.1. CL-9 as a ΛCDM RELHIC

We now address whether the observed CL-9's column density profile is consistent with the system being a RELHIC. To this end, we consider RELHICs embedded within an NFW DM halo, a profile characterized by the halo concentration and virial mass. These two parameters fully specify the RELHICs' total H I mass, central density, and characteristic size.

Therefore, we construct a grid of models as a function of virial mass and concentration, imposing the Ludlow et al. (2016) mass–concentration relation. We place the models at a fiducial distance of M94, $d = 4.66$ Mpc, and convolve them with the FAST Gaussian beam. We then adopt the best model as the model that matches CL-9's column density at the location of the second innermost isocontour, i.e., the highest signal-to-noise isocontour that has a reliable distance estimate from the center.

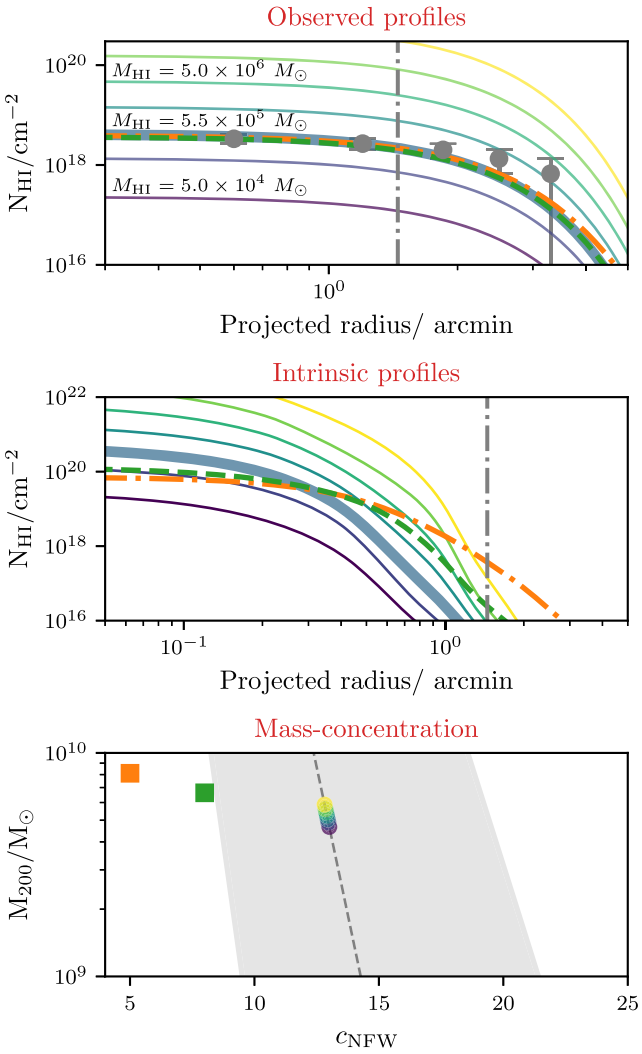

Figure 2. Top panel: CL-9's observed column density profile (circles), including 3σ uncertainties, together with mock-observed RELHICs (lines) at the distance of M94 and convolved with the FAST Gaussian beam. RELHICs were chosen to bracket CL-9's observations while following the ΛCDM mass–concentration relation. The thick line highlights the best-fit model (see text for discussion), and the labels indicate the total H I mass of the model immediately below. Middle panel: intrinsic column density profiles of the models shown in the top panel. The vertical line indicates the radial extent of the FAST beam. Bottom panel: mass–concentration relation of the models, together with the Ludlow et al. (2016) mass–concentration relation (line) and scatter (shaded region). The orange and green squares indicate examples with lower-than-average concentrations that also match observations (see the lines of the same color in the middle and top panels).

We show the model results, compared with CL-9's observation, in the top panel of Figure 2. The thin curves show examples of ΛCDM RELHICs within a very narrow range of halo mass centered at the mass of the best RELHIC model (thick line).

Three outcomes of this exercise deserve particular attention. First, it is remarkable that it is possible to match CL-9's isocontours by varying solely the halo mass of a RELHIC at the distance of M94 without further adjustments. Second, if CL-9 is indeed a RELHIC, its observed column density profile imposes a tight constraint on the mass of its DM halo, as small departures in halo mass relative to the best model produce models whose central column density quickly departs from observations. This implies that the derived properties are not

very sensitive to the comparison between the model and observations at the adopted isocontour. Third, the best RELHIC model contains an H I mass, $M_{\rm HI} \sim 5.5 \times 10^5\ M_\odot$, which is in excellent agreement with the value derived by Z23 for CL-9.[5] In contrast, other models contain H I masses that significantly depart from the inferred value, as indicated by the labels in the top panel of Figure 2. This demonstrates that CL-9 is fully consistent with a RELHIC even if it was considered an unresolved source.

We thus conclude that, if CL-9 is at the distance of M94, then its total H I mass and column density profile properties are fully consistent with a ΛCDM RELHIC of mass $M_{200} \sim 5.04 \times 10^9\ M_\odot$ and concentration $c_{\rm NFW} = 12.94$.

Although the best ΛCDM RELHIC shown by the thick solid line in Figure 2 is consistent with observations, there are slight but systematic differences between the best-fit model and observations at larger radii. A priori, these could originate from: (1) CL-9 inhabiting a DM halo with lower-than-average concentration; (2) a wrong distance estimate to CL-9; and (3) departures of the structure of the DM halo compared to ΛCDM expectations.

To address the first possibility, we constructed models with a lower-than-average concentration that match the second innermost CL-9's isocontour. The orange and green squares in the bottom panel of Figure 2 show two extreme examples. Lowering the concentration increases the halo mass, but only mildly, demonstrating that the leading factor determining the central column density of RELHICs is the DM mass. In addition, the "observed" models are only marginally more extended than the fiducial best-fit ΛCDM RELHIC (see the dashed and dotted–dashed lines in the top and middle panels), indicating that halo concentration cannot resolve the tension between modeling and observations if CL-9 is at the distance of M94.

We explore the other two possible sources of discrepancies in the following sections.

3.2. Is CL-9 a ΛCDM RELHIC Closer than M94?

If CL-9 is indeed a ΛCDM RELHIC, the systematic difference between the model and observations in the outer regions may simply reflect a wrong distance estimate for CL-9; RELHICs would appear more extended in projection and be more consistent with CL-9 if we place the system closer to the observer.

To explore the possibility that CL-9 is much closer than M94, we varied the distance to CL-9 and found that bringing the system to a distance $d = 500$ kpc from us improves the quality of the fit while still adopting the mean ΛCDM mass–concentration relation. This is shown in the top panel of Figure 3, which is analogous to Figure 2 but assumes $d = 500$ kpc.

Although this smaller distance improves the agreement between the model and observations, it is disfavored by CL-9's high recessional velocity, as discussed in Section 2.1. Placing CL-9 much farther would only increase its neutral hydrogen mass without improving the fit to observations. As shown by BL17, RELHICs should have an H I mass, $M_{\rm HI} \lesssim 3 \times 10^6\ M_\odot$, which places an upper limit to CL-9's distance, $d_{\rm CL9} \lesssim 10$ Mpc, if the system is indeed a RELHIC.

[5] CL-9's integrated flux is $S_{21} = 0.14 \pm 0.02$ Jy km s^{-1} (Z23), implying an H I mass, $M_{\rm HI} \sim (7.2 \pm 1) \times 10^5\ M_\odot$ at the M94 distance.

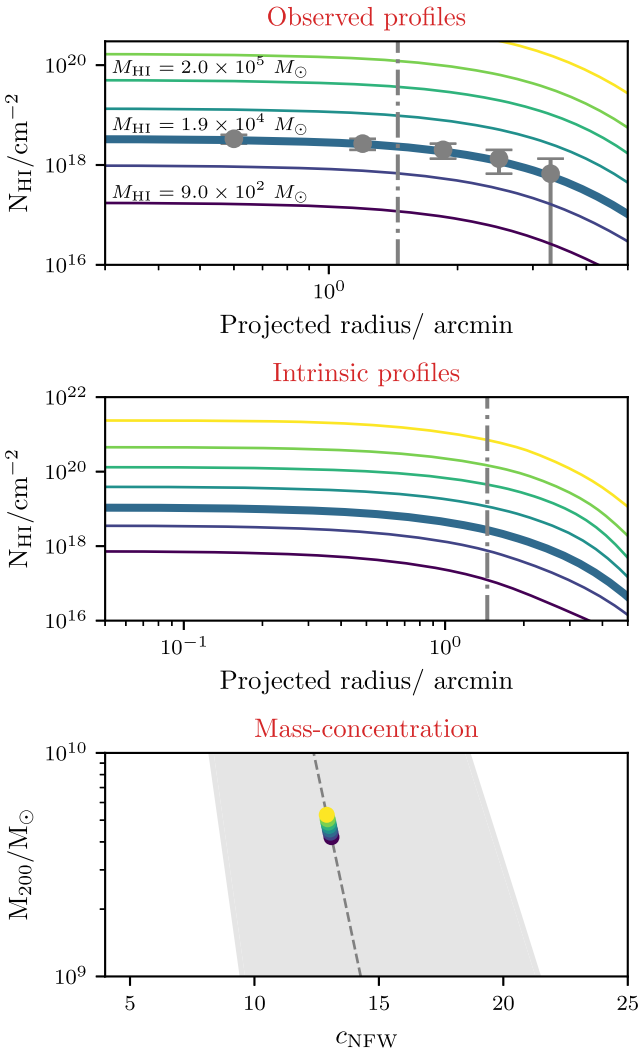

Figure 3. Identical to Figure 2, but assuming CL-9 is at a distance $d = 500$ kpc.

Finally, changes in the distance estimate of CL-9 only have a minor impact on the derived DM halo parameters. Although we have changed CL-9's distance by almost an order of magnitude between Figures 2 and 3, the resulting DM mass of the best model remains similar between the two models. It is now $M_{200} = 4.5 \times 10^9\ M_\odot$ ($c_{\rm NFW} = 13.02$). This is because RELHICs' neutral hydrogen density is extremely sensitive to halo mass, thus making the distance a secondary parameter in the explored range. This is not the case for the H I mass, which depends on distance. The inferred H I mass for CL-9 at this lower distance is $\sim(7 \pm 1) \times 10^3\ M_\odot$, which is similar to the total H I mass of the best-fit model.

Thus, we conclude that, in the unlikely scenario in which CL-9 is as close as 500 kpc from us, it would still be possible to find a ΛCDM RELHIC that matches its observed column density. In addition, the maximum allowed distance for CL-9 to contain an H I mass compatible with the system being a RELHIC is $d \sim 10$ Mpc, a distance at which CL-9 would still be compatible with a ΛCDM RELHIC.

3.2.1. Does CL-9 Signal an Inner DM Deficit?

An alternative interpretation of the systematic discrepancy between the modeling and observations in the outer regions is

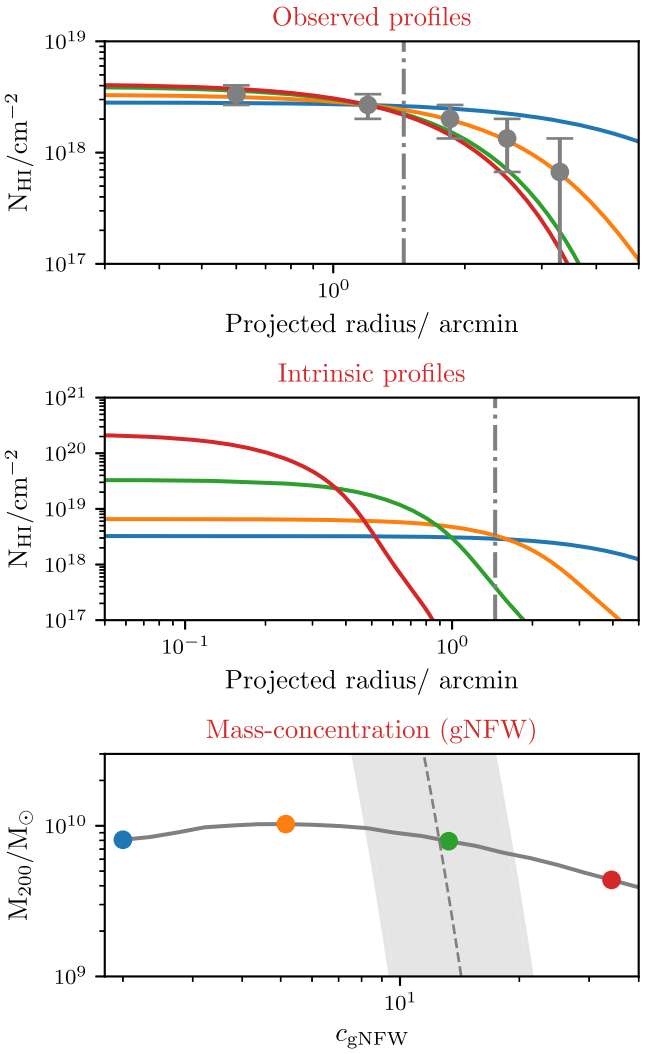

Figure 4. Identical to Figure 2, but assuming RELHICs are embedded within gNFW halos with $\gamma = 0$. See Equation (1). The solid line in the bottom panel shows the family of models that provide a good fit to the second innermost isocontour.

that it originates from a deficit of DM relative to a cuspy NFW in the inner regions. To explore this possibility, we now focus on a different model in which the gas in the halo is in hydrostatic equilibrium with a generalized NFW (gNFW) halo, whose logarithmic slope in the inner regions, γ, is treated as a free parameter:

$$\rho_{\rm dm}(r) = \rho_s \left(\frac{r}{r_s}\right)^{-\gamma} \left[1 + \left(\frac{r}{r_s}\right)\right]^{\gamma-3}. \quad (1)$$

To impose a deficit of DM in the center relative to a cuspy NFW, we enforce a cored inner density profile by setting $\gamma = 0$. We consider a grid of RELHIC models, for which we vary both the halo mass and concentration independently of each other. We then fit the models, placed at the same distance of M94 and convolved with the FAST beam, to CL-9's second innermost isocontour. The result of this procedure is shown in Figure 4.

With these changes, a RELHIC inhabiting a "cored" DM halo of mass, $M_{200} \sim 1.02 \times 10^{10}\ M_\odot$, and concentration, $c_{\rm gNFW} = r_{200}/r_s = 5.15$, matches observations (see the orange line in the top panel of Figure 4). Other models, found by

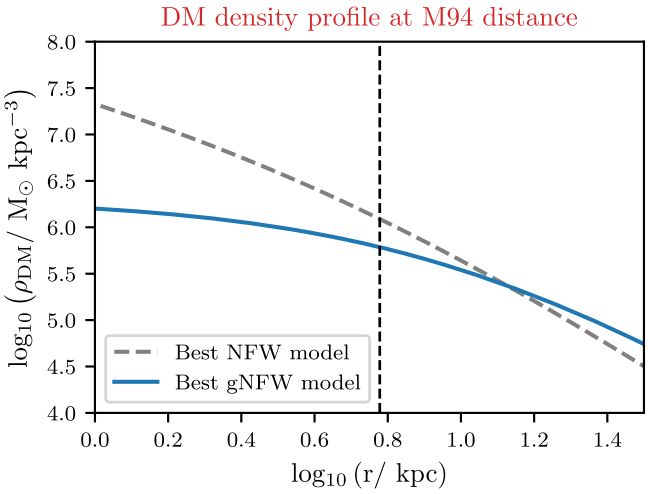

Figure 5. Mean DM density profile of the best-fit ΛCDM RELHIC model at the fiducial distance of M94 (gray dashed line) compared with the best-fit gNFW RELHIC model. The DM content between the models differs by more than a factor of 2 below ∼6 kpc (vertical line).

varying both the halo mass and concentration until they match the central column density, fit the observed profile very poorly. Although the concentration of the best model is off of the Ludlow et al. (2016) mass–concentration relation (shown in the bottom panel of Figure 4), there is no reason why a cored profile should follow this relation.

The derived halo parameters thus imply a significant DM mass deficit greater than a factor of 2 for radii, $r \lesssim 6$ kpc compared to ΛCDM expectations. This is shown in Figure 5, in which we plot the mean DM density profile of the best ΛCDM RELHIC and the best gNFW RELHIC. These parameters are uncomfortably large compared with the values expected from self-interacting DM (SIDM) models and difficult to reconcile with ΛCDM without a bright stellar counterpart. For example, Elbert et al. (2015) found that the largest radius at which SIDM halos depart from ΛCDM is roughly a factor 3 smaller (∼2 kpc). In addition, if CL-9 hosted a stellar counterpart, its low stellar mass would make it difficult for supernova-driven winds to perturb its inner DM at such large distances (e.g., Di Cintio et al. 2014; Tollet et al. 2016; Robles et al. 2017). Therefore, if CL-9 is confirmed to be a RELHIC and further observations confirm the extended mass deficit, we anticipate challenges reconciling this system not only with the ΛCDM model but also with SIDM models.

4. Summary and Conclusions

In this work, we explored whether the recently discovered extended H I gas cloud CL-9 is consistent with being a ΛCDM RELHIC. We find that CL-9's properties are consistent with the system being a RELHIC, as recently argued by Z23. The match between the model column densities and observations, together with the large projected distance between CL-9 and M94, the round shape of CL-9's isocontours, the lack of a luminous counterpart, the small broadening of the emission line, and the total H I mass make CL-9 the first firm RELHIC candidate in the local Universe. The analysis of this system demonstrates the potential of these objects as cosmological probes.

We also find that CL-9's observations are limited by the FAST beam, the size of which is comparable to that of the

expected H I core of the most massive RELHICs at the fiducial distance. However, given the high sensitivity of the column density (and total H I mass) to halo mass for RELHICs, we conclude with high confidence that the observed system must inhabit a DM halo with mass in the range $4 \times 10^9 \lesssim M_{200}/M_\odot \lesssim 5 \times 10^9$ if its DM content follows a cuspy NFW profile. This conclusion is based on matching CL-9's total H I mass (and central column density) and, therefore, is independent of whether the system is marginally resolved or unresolved.

Taken at face value, the marginally resolved CL-9 column density profile is systematically more extended than expected for a ΛCDM RELHIC. If confirmed, this may suggest a slightly more massive halo, $M_{200} \sim 10^{10}\, M_\odot$, but with a large inner core rather than a cusp. However, before drawing robust conclusions, it is crucial to observe CL-9 with higher spatial resolution.

We envision a series of observations that may help constrain CL-9's parameters and nature. First, the high sensitivity and smaller beam make the MeerKAT radio telescope an obvious choice to constrain CL-9's column density profile better. However, the high decl. of CL-9 ($\delta \sim +40°$) places the system at the limit of what can be observed with MeerKAT. CL-9 is also at the reach of the Very Large Array, an instrument that would increase the spatial resolution of the observed profile. In addition, further observations with FAST may help decrease the beam's impact.

Second, the derived halo mass for CL-9 makes the system an excellent candidate to look for the predicted RELHICs' ring-shaped Hα emission counterparts (Sykes et al. 2019). These observations could be performed with narrowband Hα filters on the Dragonfly Telephoto Array (Abraham & van Dokkum 2014) and would provide data to constrain further the system's DM content and the local intensity of the UVB.

Third, follow-up observations with the Hubble Space Telescope that go fainter than the limit of the DESI LS may help to elucidate whether CL-9 has a luminous counterpart.

Finally, observations of bright background sources that intersect CL-9 could help characterize the system's metallicity, thus helping to constrain the likelihood of CL-9 hosting a stellar counterpart.

There is a high probability that CL-9 contains a luminous galaxy in its center. At the inferred mass, we expect more than 90% of the halos to host galaxies (see, e.g., Sawala et al. 2016; BL17; Benitez-Llambay & Frenk 2020). Detecting a stellar counterpart would help constrain and break the current degeneracies and assess the quality of our predictions.

Regardless of whether or not CL-9 has a stellar counterpart, its low stellar content, together with its H I reservoir, will still allow us to put joint constraints on its underlying DM distribution. Pursuing this path, although arduous, may be highly rewarding in the end. It will provide a unique opportunity to challenge the ΛCDM model and our fundamental understanding of how galaxies form at the smallest scales.

Acknowledgments

We thank the anonymous referee for a constructive review that helped improve our presentation. A.B.L. acknowledges support from the European Research Council (ERC) under the European Union's Horizon 2020 research and innovation program (GA 101026328).

ORCID iDs

Alejandro Benitez-Llambay https://orcid.org/0000-0001-8261-2796
Julio F. Navarro https://orcid.org/0000-0003-3862-5076

References

Abraham, R. G., & van Dokkum, P. G. 2014, PASP, 126, 55
Adams, E. A. K., Giovanelli, R., & Haynes, M. P. 2013, ApJ, 768, 77
Angulo, R. E., Springel, V., White, S. D. M., et al. 2012, MNRAS, 426, 2046
Benitez-Llambay, A., & Frenk, C. 2020, MNRAS, 498, 4887
Benítez-Llambay, A., Navarro, J. F., Frenk, C. S., et al. 2017, MNRAS, 465, 3913
Blumenthal, G. R., Faber, S. M., Primack, J. R., & Rees, M. J. 1984, Natur, 311, 517
Bond, J. R., Cole, S., Efstathiou, G., & Kaiser, N. 1991, ApJ, 379, 440
Bromm, V., & Yoshida, N. 2011, ARA&A, 49, 373
Bullock, J. S., & Boylan-Kolchin, M. 2017, ARA&A, 55, 343
Cappellari, M., Emsellem, E., Krajnović, D., et al. 2011, MNRAS, 413, 813
Crook, A. C., Huchra, J. P., Martimbeau, N., et al. 2007, ApJ, 655, 790
Di Cintio, A., Brook, C. B., Macciò, A. V., et al. 2014, MNRAS, 437, 415
Elbert, O. D., Bullock, J. S., Garrison-Kimmel, S., et al. 2015, MNRAS, 453, 29
Ferrero, I., Abadi, M. G., Navarro, J. F., Sales, L. V., & Gurovich, S. 2012, MNRAS, 425, 2817
Graziani, R., Courtois, H. M., Lavaux, G., et al. 2019, MNRAS, 488, 5438
Haardt, F., & Madau, P. 2012, ApJ, 746, 125
Haynes, M. P., Giovanelli, R., Kent, B. R., et al. 2018, ApJ, 861, 49
Hoeft, M., Yepes, G., Gottlöber, S., & Springel, V. 2006, MNRAS, 371, 401
Ikeuchi, S. 1986, Ap&SS, 118, 509
Jenkins, A., Frenk, C. S., White, S. D. M., et al. 2001, MNRAS, 321, 372
Karachentsev, I. D., & Kaisina, E. I. 2019, AstBu, 74, 111
Karachentsev, I. D., Kaisina, E. I., & Makarov, D. I. 2018, MNRAS, 479, 4136
Karachentsev, I. D., Karachentseva, V. E., Huchtmeier, W. K., & Makarov, D. I. 2004, AJ, 127, 2031
Kourkchi, E., Courtois, H. M., Graziani, R., et al. 2020, AJ, 159, 67
Lee, J. C., Gil de Paz, A., Kennicutt, R. C., Jr., et al. 2011, ApJS, 192, 6
Ludlow, A. D., Bose, S., Angulo, R. E., et al. 2016, MNRAS, 460, 1214
Martínez-Delgado, D., Roca-Fàbrega, S., Miró-Carretero, J., et al. 2023, A&A, 669, A103
Navarro, J. F., Frenk, C. S., & White, S. D. M. 1996, ApJ, 462, 563
Okamoto, T., Gao, L., & Theuns, T. 2008, MNRAS, 390, 920
Press, W. H., & Schechter, P. 1974, ApJ, 187, 425
Rahmati, A., Pawlik, A. H., Raičević, M., & Schaye, J. 2013, MNRAS, 430, 2427
Rees, M. J. 1986, MNRAS, 218, 25P
Robles, V. H., Bullock, J. S., Elbert, O. D., et al. 2017, MNRAS, 472, 2945
Sawala, T., Frenk, C. S., Fattahi, A., et al. 2016, MNRAS, 456, 85
Shaya, E. J., Tully, R. B., Hoffman, Y., & Pomarède, D. 2017, ApJ, 850, 207
Sykes, C., Fumagalli, M., Cooke, R., Theuns, T., & Benítez-Llambay, A. 2019, MNRAS, 487, 609
Tollet, E., Macciò, A. V., Dutton, A. A., et al. 2016, MNRAS, 456, 3542
Tully, R. B., Courtois, H. M., & Sorce, J. G. 2016, AJ, 152, 50
Wang, J., Bose, S., Frenk, C. S., et al. 2020, Natur, 585, 39
Zhou, R., Zhu, M., Yang, Y., et al. 2023, ApJ, 952, 130